https://doi.org/10.15407/ujpe70.1.24

Z. BARANCHYKOV, YU. HIZHNYI, O. MAKARENKO, S.G. NEDILKO
Kyiv National University named after Taras Shevchenko
(64/13, Volodymyrska Str., Kyiv 01601, Ukraine; e-mail: zahares4731@gmail.com)

ELECTRONIC STRUCTURE AND POSSIBILITY OF EXPERIMENTAL MONITORING OF THE PHASE COMPOSITION OF POLYVINYLIDENE FLUORIDE (PVDF) CRYSTALS

The organic polymer polyvinylidene fluoride (PVDF) is a promising and commercially attractive material for the modern needs of nanotechnology and microelectronics and biomedicine. Detecting the phase composition of PVDF blends is an important technological task. This paper presents the results of ab initio calculations of the electronic band structure of the three most common phases of polyvinylidene fluoride crystals α-, β- and γ-PVDF. The band dispersion curves, partial densities of electronic states, spatial distributions of electronic densities, spectra of dielectric constants, complex refractive index, absorption and reflection, infrared absorption spectra, Raman scattering and X-ray diffraction patterns of α-, β- and γ-phases of PVDF were obtained and analyzed. Analysis of the results of electronic structure calculations allowed to draw a number of conclusions regarding the peculiarities of formation of electronic and optical properties of the α-, β-, and γ-phases of PVDF crystal, as well as to make some predictions about the possibility of experimental monitoring of the phase composition of this compound. It has been established that detection of the simultaneous presence of β- and α- (or γ-) phases in PVDF crystal samples can be effectively performed by vacuum ultraviolet reflection spectroscopy, infrared absorption, Raman spectroscopy, and X-ray diffraction analysis. The presence of the α- phase on the background of the γ-phase of PVDF will be practically impossible to detect using these methods.

Keywords: polyvinylidene fluoride, crystal, electronic structure, optical spectra, phase composition.

1. Introduction

First synthesized in 1948, poly(vinylidene fluoride) (PVDF) is known for its chemical resistance, mechanical strength, and flame retardancy. This makes it the most widely used high-performance engineering plastic for architectural, industrial, automotive, and pharmaceutical applications. Further research has shown that PVDF films exhibit a strong piezoelectric effect [1]. This has led to its use as a piezoelectric organic polymer that can compete [2] with inorganic piezoelectrics in nanotechnology and microelectronics [3, 4]. Due to its high compatibility with many biological molecules and tissues, PVDF is a promising material in bio- and nanomedicine [5–9].

Citation: Baranchykov Z., Hizhnyi Yu., Makarenko O., Nedilko S.G. Electronic structure and possibility of experimental monitoring of the phase composition of polyvinylidene fluoride (PVDF) crystals. *Ukr. J. Phys.* **70**, No. 1, 24 (2025). https://doi.org/10.15407/ujpe70.1.24.

The chemical structure of PVDF contains a repeating unit of doubly fluorinated ethane CH_2–CF_2. Each unit has a dipole moment of 7×10^{-30} Kl $\cdot$ m associated with positively charged hydrogen atoms and negatively charged fluorine atoms. Since these dipoles are rigidly attached to the main carbon chain, their orientation is directly controlled by the conformation and packing of the molecules. PVDF forms four polymorphic crystalline phases, which are determined by the conformation of the polymer chains and their steric order (crystal structure).

The possibility of the existence of PVDF in four crystalline phases – α, β, γ and δ – has been confirmed so far [10, 11]. In addition, the existence of the ε- phase has been predicted [12]. With a parallel arrangement of dipoles in the polymer chain, the crystal in the polar β, γ, and δ phases has a significant resulting dipole moment. With an antiparallel arrangement in the polar α and ε phases, the resulting dipole moment almost disappears.

The main crystalline form of PVDF is the α-phase, which is mainly formed during crystallization from the melt when it is supercooled [13], as well as during polymerization. The α-phase is nonpolar and has no ferroelectric properties.

Under the influence of heat, mechanical stress, or an electric field, the α-phase can be transformed into other phases. The most important polymorphic phase of PVDF, which is widely used for piezoelectric and pyroelectric applications, is the β-phase, which is usually obtained from the α-phase during mechanical deformation [14]. It is this complete trans-conformation of the β-phase that determines its ferroelectric properties.

The γ-phase was obtained by crystallization from solutions [15], at high pressures [16], at high temperatures [17], and after annealing the α-phase of PVDF [18]. The γ-phase of the polymer has ferroelectric properties that are intermediate between those of the α- and β-phases.

The ferroelectric δ-phase can be formed when the α-phase is polarized by an electric field [19]. The δ-phase has the same macromolecular chain conformation and unit cell size as the α-phase, the only difference being the packing of the polymer chains.

A real PVDF polymer is almost always a mixture of several polymorphic phases that are difficult to separate. Detecting the phase composition of such mixtures is an important technological task. For their identification, experimental methods such as X-ray diffraction [20, 21], infrared spectroscopy (FTIR) [13, 22, 23], Raman scattering [24], and nuclear magnetic resonance (NMR) [23] are used. However, this identification can only be successful if the physical properties of all phases that make up the mixture are known. These properties can be obtained by calculating the electronic structure from first principles.

This paper presents the results of *ab initio* calculations of the electronic band structure of the three most common phases of polyvinylidene fluoride crystals, known in the literature as α-, β- and the γ-phase of PVDF. The structure of the single-electron bands (band dispersion curves), partial densities of electronic states, spatial distributions of electronic densities, spectra of dielectric constants, complex refractive index, absorption, and reflection of the three mentioned phases of PVDF crystal were obtained and analyzed. Using the DFT electronic structure method, the infrared absorption and Raman spectra of α-, β- and γ-phases of PVDF were calculated, and the angular distributions of X-ray diffraction (XRD) were obtained from the geometrically optimized atomic structure of these compounds.

The obtained calculation results are analyzed in terms of possible monitoring of the phase composition of PVDF crystals. The calculations show that the α- and γ-phases of PVDF are characterized by a very similar electronic structure and related characteristics, while the corresponding properties of the β- phase differ significantly from the case of α- (or γ). Therefore, the detection of the simultaneous presence of β- and α- (or γ) phases in PVDF crystal samples can be effectively performed by vacuum ultraviolet reflectance spectroscopy, infrared absorption, Raman, and XRD analysis. The presence of the α-phase on the background of the γ-phase of PVDF will be practically impossible to detect using these methods.

The electronic structure of PVDF crystals has been previously calculated by various methods [25, 26, 27], while a systematic comparison of the electronic structure and related properties of α-, β- and γ phases of a polyvinylidene fluoride crystal was performed for the first time in this work.

2. Calculation Methodology

In the calculations, we used the well-known crystal structures of the three phases of PVDF crystals found in the literature [28]. The corresponding structural data are given in Table.

The electronic structure of the α-,β- and γ-phases of PVDF crystals was calculated by the band-periodic DFT method of the plane-wave basis set pseudopotential, which is implemented in the CASTEP package [29]. In these calculations, ion-electron interactions were modeled by nonlocal pseudopotentials of the Vanderbilt type [30]. Exchange-correlation effects were taken into account in the GGA approximation using the PBE potential approximation [31]. The energy threshold defining the size of the plane wave basis was 761.9 eV. The nuclei geometry was optimized using the Broyden–Fletcher–Goldfarb–Shenno (BFGS) minimization technique [32] using the criterion of simultaneous convergence in energy and force on atoms, which were 10^{-5} eV per atom and 0.03 eV/Å per atom, respectively.

Using the methods implemented in the CASTEP package [29], we calculated the dispersion curves $E(k)$ (one-electron bands) of crystals, the partial densities of the electronic states (PDOS) of atoms of unit cells, the spectra of optical constants (real and imaginary parts of the dielectric constant tensor, refractive index, and absorption), and the spectra of optical absorption and reflection using well-known relations. The spectra of optical constants were calculated for the condition of normal incidence, the approximation of the coincidence of the optical axes of crystals with the crystallographic axes, and the condition of polycrystallinity of the crystal (averaging over spatial coordinates). Further details on the applied approximations can be found in the authors' previous work [33].

Structural parameters of α-, β- and γ-phase PVDF crystals used in the calculations

Phase	Symmetry group (number and symbol)	Lattice parameters	Volume of the unit cell, Å^3
α	14 P2/c$_1$	$a = 4.45868$ Å $b = 8.44829$ Å $c = 4.54252$ Å $\alpha = \gamma = 90°$ $\beta = 91.4895°$	171.11
β	38 Amm2	$a = 2.53619$ Å $b = 7.73382$ Å $c = 4.22311$ Å $\alpha = \beta = \gamma = 90°$	82.83
γ	33 Pna2$_1$	$a = 4.51162$ Å $b = 8.49118$ Å $c = 4.53377$ Å $\alpha = \beta = \gamma = 90°$	173.68

The density functional perturbation theory (DFPT) implemented in CASTEP was used to obtain the phonon spectrum and vibrational properties. The angular dependences of the X-ray diffraction intensity were calculated using the auxiliary utility Forcite Plus.

3. Results and Discussion

The structures of the unit cells of α-, β-, and γ-phases of a PVDF crystal are shown in Fig. 1. As can be seen from the figure, the structures of the α- and γ-phases are generally similar, while the structure of the β-phase differs significantly from the α (or γ) case. The α- and γ-phases have virtually the same chain structure ...–CH_2–CF_2–CH_2–... and differ only in their relative arrangement. Due to this difference, the α- and γ-phases are characterized by different configurations of "interchain" distances H–F (shown in Fig. 1, *a* and *c* by dashed lines).

Instead, the β-phase of the PVDF crystal has a completely different chain structure: the CH_2 and CF_2 elements are arranged so that the chain element contains three C atoms, and they all lie in the same plane. In the case of $\alpha(\gamma)$, the structure of the chain element is more complicated – it contains four C atoms that do not lie in the same plane (compare Fig. 1, *a* and *b*).

As will be shown later in this paper, this similarity between the structures of α and β and the significant difference between the cases of β and $\alpha(\gamma)$ also determines the similarities and differences in the electronic structure and optical characteristics of different phases of the PVDF crystal.

The calculated X-ray diffraction patterns of the three phases of the PVDF crystal are shown in Fig. 2. As can be seen from the figure, the XRD patterns of the α- and γ-phases differ significantly from the β-phase. In the case of the β-phase, there are no intense lines at angles $2\theta = 20$, 30, 45, and 53°, which are present in the XRD patterns of the α- or γ-phase. The difference between the α- and γ-phase XRDs is much smaller, but nevertheless noticeable. In partic-

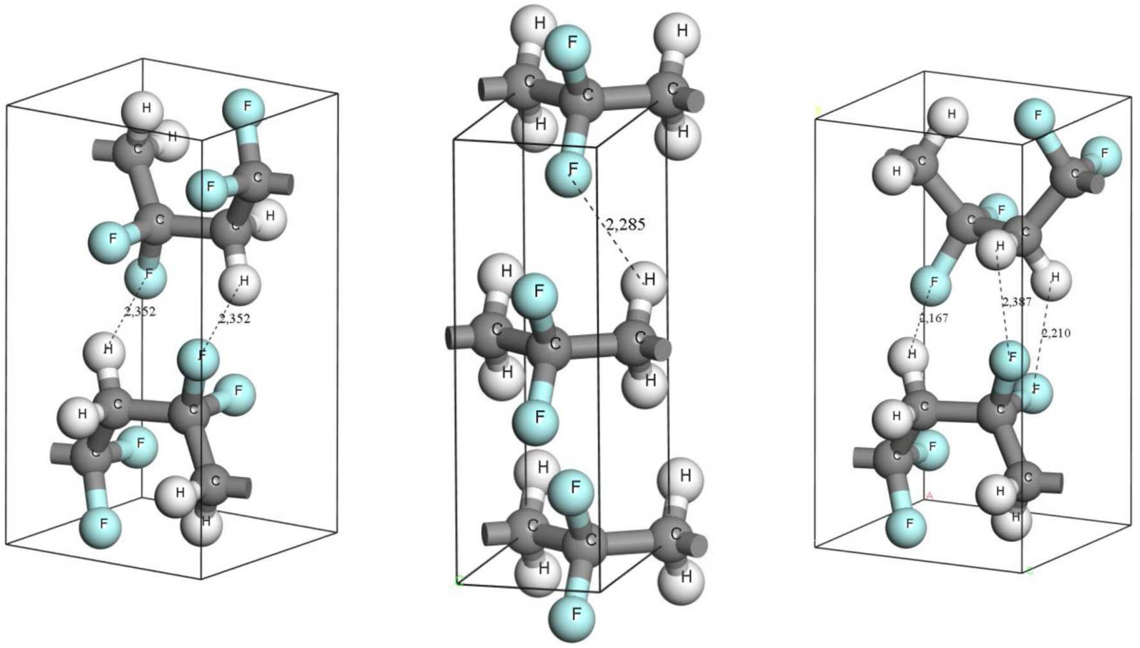

a *b* *c*

Fig. 1. The structure of the unit cells of α- (a), β- (b), and γ-phase of a PVDF crystal (c)

ular, the α-phase has characteristic lines at 20 and 35°, which are absent in the case of γ.

Thus, our calculations suggest that it will be quite easy to distinguish the $\alpha(\gamma)$ phase of a PVDF crystal from the β phase in XRD experiments, while it will be more difficult to distinguish α from γ, although possible in principle.

The calculated band structure (dispersion curves $E(k)$ or one-electron bands) of the three phases of the PVDF crystal is shown in Fig. 3. The dispersion curves $E(k)$ were calculated on the segments connecting the characteristic points of the first Brillouin zone of the symmetry groups, which are given in Table. The starting point of the energy scale in this figure is chosen from the position of the calculated Fermi level E_{F}. For all three phases of the crystal, the Valence bands (VB) are in the energy range from –13 to 0 eV. The calculated values of the energy gaps E_g are 7.27, 6.30, and 7.20 for the α-, β-, and γ-phases, respectively. As our calculations show, all three PVDF phases are direct-band crystals, since the lowest energy band transition can occur without changing the value of the quasi-momentum $\mathbf{k}$ (at point Γ, which corresponds to the center of the first Brillouin zone, see Fig. 3).

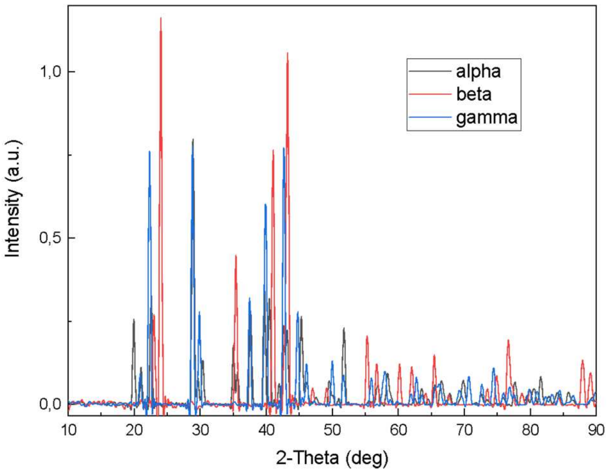

Fig. 2. Calculated angular dependences of the X-ray diffraction intensity (diffractograms) of the α-, β-, and γ-phase of the PVDF crystal (black, red, and blue curves, respectively)

As can be seen from Fig. 3, the band structures of the α- and γ-phases are so similar that it is difficult to distinguish them, especially in the VB energy region. However, there is a certain difference, and it is reflected in the calculated PDOS: the most intense

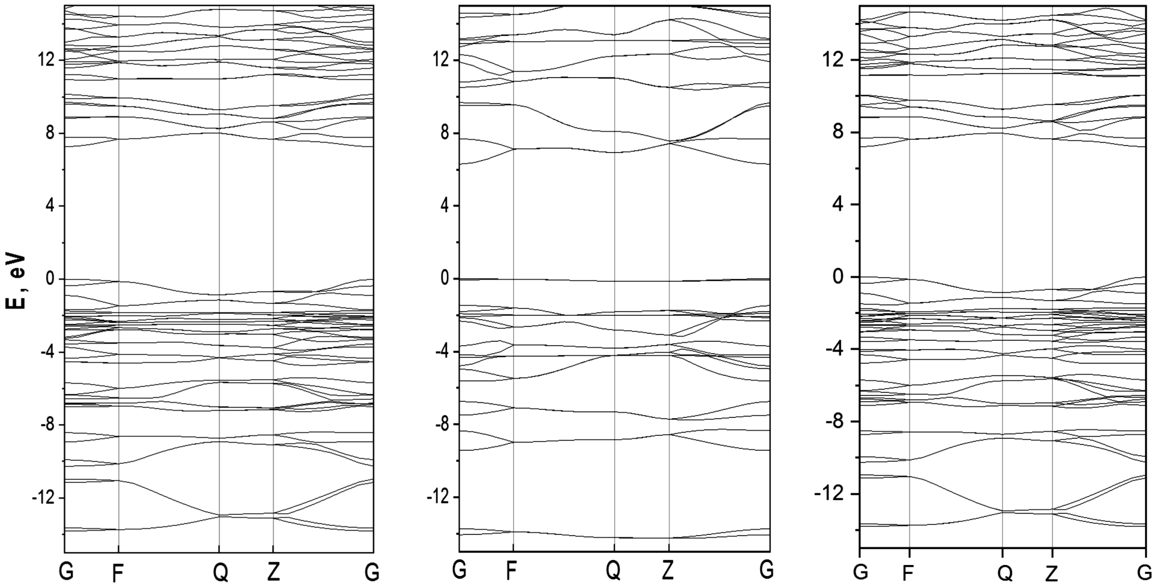

a *b* *c*

Fig. 3. The calculated band structure of α- (*a*), β- (*b*), and γ-phase PVDF crystals (*c*)

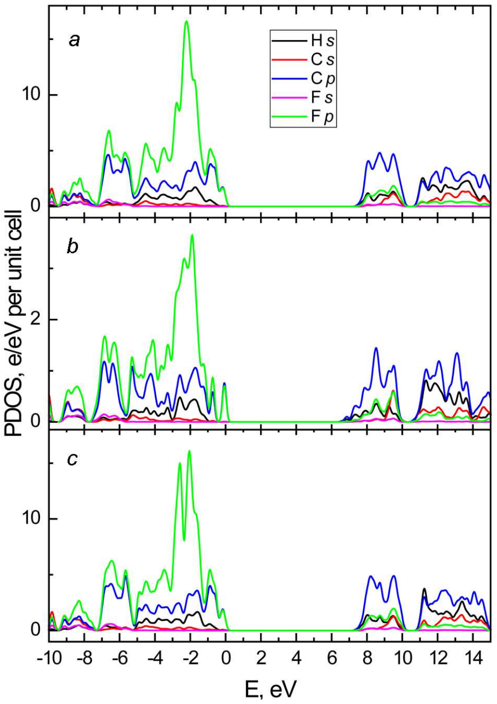

Fig. 4. Calculated partial densities of electronic states of the α- (*a*), β- (*b*), and γ-phase (*c*) of the PVDF crystal

peaks of the density of states F_p of α and γ phases are at different energies (see Fig. 4, *a* and *c*).

As can be seen from Fig. 3, the β-phase of PVDF crystal has a significantly different configuration of the dispersion curves $E(k)$ in the VB region compared to the $\alpha(\gamma)$ case. The main difference in the band structure of the β-phase is the presence of a monodispersed one-electron band near 0 eV, which is separated from other one-electron bands of the valence band by an empty (without states) energy band with a width of $\sim$1.5 eV. As can be seen from the PDOS distributions (see Fig. 4, *b*), this separated one-electron band is formed by the C_p and F_p orbitals, with the contribution of both of these types of states being equal. The same picture is observed in the case of α- and γ-phases: the top of the VB is formed by C_p and F_p states in equal proportions (see Fig. 4, *a*, *c*).

Figure 4 also clearly shows that for all three phases, the top of VB (TVB) lacks H_s states, and at the bottom of the Conduction band (BCB) the C_p states dominate with minor contributions from F_p and H_s states. Thus, the electronic structure properties at the band edges (TVB and BCB) of PVDF crystals are determined mainly by the orbitals of C and F atoms. Therefore, it is not unexpected that such a structure differs significantly between the cases of the β and $\alpha(\gamma)$ phases, which have significantly different carbon chain configurations (see above).

The formation of the TVB by C_p and F_p states and the absence of H_s states there actually means that the crystal conductivity (in the case of charge carriers – holes) is most likely to occur along the chains ...–CH_2–CF_2–CH_2–... . According to the structure of all three phases of the PVDF crystal (see Fig. 1), the "interchain" chemical bonds involve H atoms whose orbitals do not participate in the formation of the TVB, and therefore there should be no regions of high electron density in the "interchain" space that cause hole conductivity.

In order to analyze this issue in more detail, we calculated the spatial distributions of the electron density at the TVB and BCB of the three phases of the PVDF crystal (Fig. 5). In the case of the TVB, for the α- and γ-phases, the spatial electron density of the two highest filled single-electron zones of the crystal is summarized in the calculations, while for the β-phase, only one, highest filled zone is summarized. This is due to the fact that the band gap of the α- and γ-phases is formed by two one-electron bands that are difficult to separate. Or, in other words, the band gap of the α- and γ-phases is formed by a twice degenerate one-electron band that undergoes splitting only at point Γ (see Fig. 3, *a*, *c*). For the β-phase, the situation is different – the TVB is formed by a single non-degenerate one-electron band (see Fig. 3, *b*). In the case of the BCB, for all three phases, the electron density of the lowest unfilled one-electron band is taken into account in the calculations.

As can be seen from Fig. 5 (lower half), for all three phases of the PVDF crystal, the electron density distribution at the TVB is such that it provides a significant spatial overlap of atomic orbitals along the structural chains of carbon atoms ...–C–C–C–... Such a significant overlap means that in the PVDF crystal of all three phases there should be channels of enhansed conductivity in areas where there is a significant overlap of atomic orbitals [34], i.e., along the chains ...–CH_2–CF_2–CH_2–... . (Crystallographic directions (0 0 1), (1 0 0), and (0 0 1) for the α-, β-, and γ-phases, respectively). The figure also clearly shows that in the TVB, these chains are separated from each other by spatial regions with low electron density. This means that in the directions perpendicular to the directions of the chains, the hole conductivity of all three phases will be much lower than in the directions along the chains.

As shown by the electron density distributions in the upper part of Fig. 5, there is no continuous spatial overlap of atomic orbitals at the BCBs of all three phases, both along the chains and between them. This means that electron-driven conduction should be inefficient (compared to hole conduction) for all three phases of the PVDF crystal, regardless of the direction in space.

Thus, according to the results presented in Fig. 5, our calculations suggest: a) significant anisotropy of the conductivity of the α-, β-, and γ-phases of the PVDF crystal; b) the hole type of conductivity should prevail in all these phases.

Before analyzing the calculated optical characteristics of PVDF crystals, the following should be noted. It is well known that the use of the GGA approximation with the PBE exchange-correlation functional in electronic structure calculations may lead to a significant (several eV) underestimation of the calculated dielectric band gap values E_g compared to their real values (the so-called DFT underestimation). The underestimation can lead to the fact that the calculated fundamental absorption edge and other spectral features of the optical characteristics formed by the band-band transitions will be at significantly lower energies than should be manifested in the corresponding experimental spectra. However, in this work we will not take into account such a possible discrepancy between the calculations and the experiment, since the subject of analysis is primarily the *difference* between the calculated spectral properties of the three phases of the PVDF crystal. In our case, the DFT underestimation can be considered the same for all three phases of the crystal. Therefore, the difference between the E_g values of the α-, β-, and γ-phases obtained in the calculations will obviously exclude the mentioned systematic calculation error.

The general view of the calculated spectra of dielectric constants ε_1 and ε_2 (shown in Fig. 6, *a*) fully reflects the similarity of the electronic structure of the α- and γ-phases of the PVDF crystal and the significant difference in the electronic structure of the β-phase from the $\alpha(\gamma)$ case. The spectra of both ε_1 and ε_2 of the α- and γ-phases are difficult to distinguish at the scale of Fig. 5, but the difference in the β-phase spectra is clearly visible.

The spectra of refractive indices n and absorption κ of $\alpha(\gamma)$- and β-phases of the PVDF crystal differ significantly in the spectral range above 6 eV (see

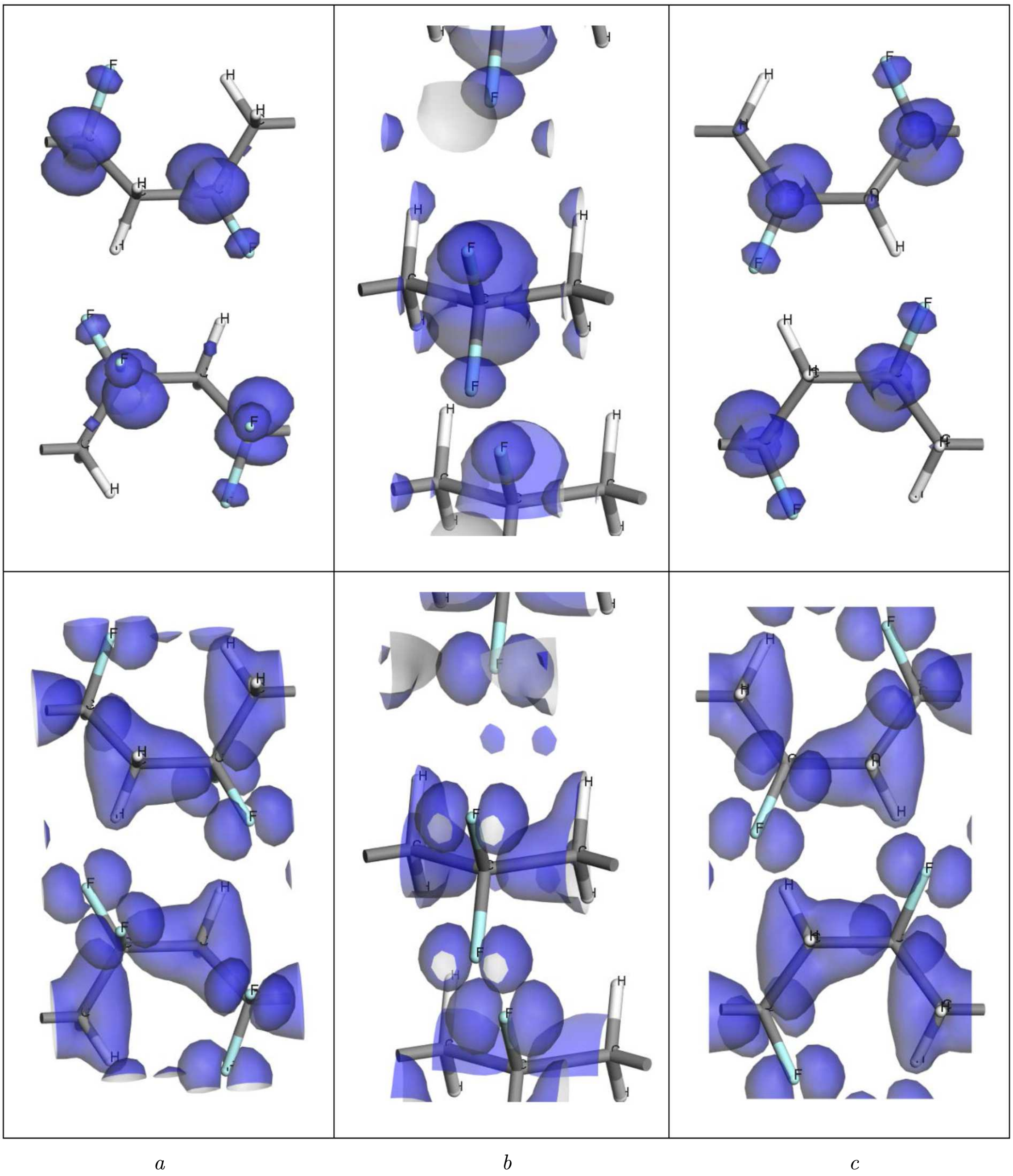

Fig. 5. Calculated spatial distributions of electron density in the energy regions of the top of the Valence band (bottom row) and the bottom the Conduction band (top row) of α- (a), β- (b), and γ-phase (c) of a PVDF crystal. The blue isosurfaces correspond to 0.04 e level of electron density

Fig. 6, b). However, as can be seen from the figure, in the spectral region of visible light (2–4 eV), the value of n of all three phases is almost the same – the difference in values is within 0.02. Such a small difference implies that it will be extremely difficult to distinguish between the α-, β-, and γ-phases of

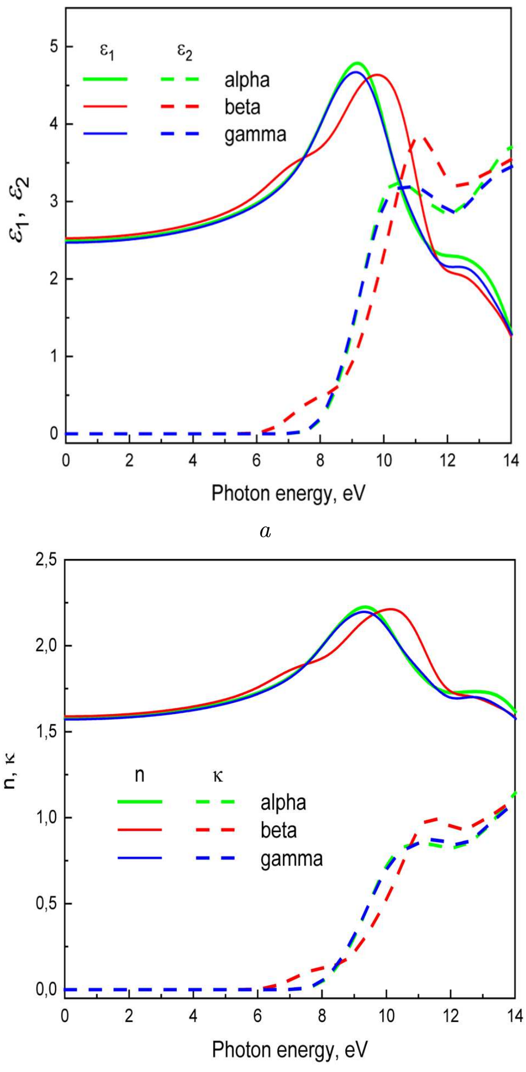

a

b

Fig. 6. Calculated spectra of: dielectric constants ε_1 and ε_2 (*a*); refractive indices *n*and absorption κ of α-, β-, and γ-phase PVDF crystals (green, red, and blue curves, respectively) (*b*)

a PVDF crystal by experimental methods of surface ellipsometry.

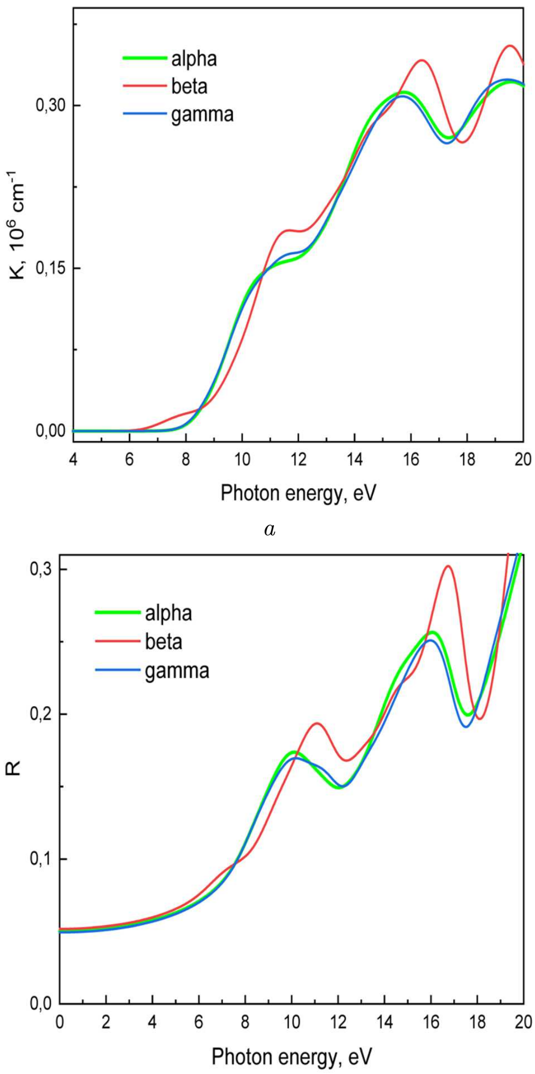

a

b

Fig. 7. Calculated absorption (*a*) and reflection (*b*) spectra of α-, β-, and γ-phase PVDF crystals (green, red, and blue curves, respectively)

The spectra of the absorption coefficient K and reflection R of the β-phase also differ significantly from the $\alpha(\gamma)$ case (see Fig. 7). As can be seen from the figure, the optical absorption of β-phase begins at much lower energies than in the $\alpha(\gamma)$ case. According to our calculations of E_g, this difference should be $\sim$1 eV (see above). This means that the difference in the absorption spectra of the β- and $\alpha(\gamma)$ phases of a PVDF crystal can be actually detected, for example, in vacuum ultraviolet reflectance experiments.

The calculated Raman spectra show that it will be practically impossible to distinguish between α and γ phases by experimental Raman spectroscopy in the Raman shift spectral region up to 1500 cm^{-1} (see black and blue curves in Fig. 8). As can be seen from the figure, all the lines in Raman spectra of these two crystal phases practically do not differ in spectral positions. However, the β-phase of PVDF has

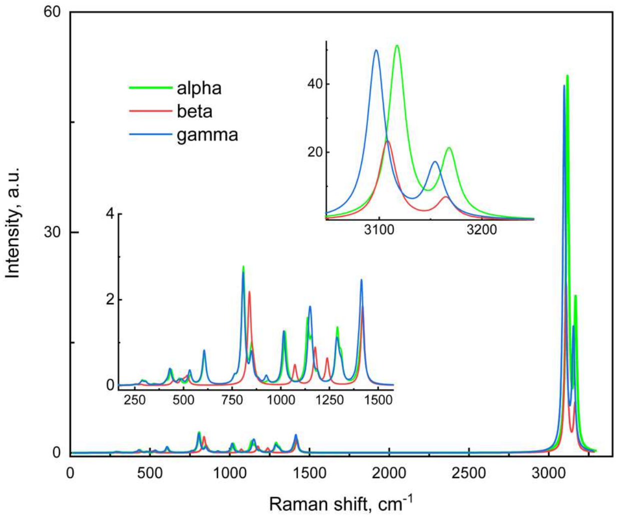

Fig. 8. Calculated Raman spectra of the α-, β-, and γ-phases of the PVDF crystal (green, red, and blue curves, respectively). The detailed structure of the spectra is shown in the insets

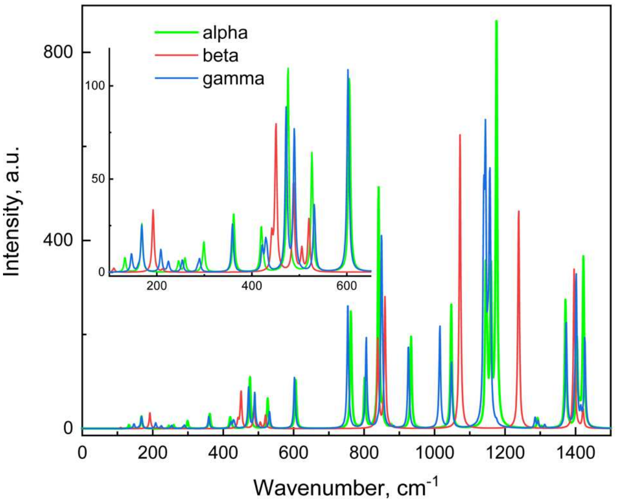

Fig. 9. Calculated infrared absorption spectra of the α-, β-, and γ-phases of a PVDF crystal (green, red, and blue curves, respectively). The inset shows the details of the spectra in the long-wave region

a significantly different Raman spectrum (red curve in Fig. 8). In particular, it contains intense lines at 1072, 1174, and 1237 cm^{-1}, which have no analogs in the corresponding spectra of the $\alpha(\gamma)$ phase. These lines have a sufficient spectral distance to the nearest neighboring $\alpha(\gamma)$-phase lines (about $\sim$50 cm^{-1}) to be easily separated in Raman spectroscopy experiments.

In the region of 3000–3300 cm^{-1} , the spectra of all three phases of the crystal differ significantly (see the corresponding inset in Fig. 8), but the difference between the spectral positions of the lines is small (not exceeding 10–20 cm^{-1}).

Similarly, using the IR absorption spectra (see Figure 9), the β-phase of PVDF crystal can be easily distinguished from the $\alpha(\gamma)$-phase. This can be done by detecting distinct spectral lines at 190 and 447 cm^{-1}, which have no analogues in the IR absorption spectra of $\alpha(\gamma)$ phases. Obviously, such detection can only be realized if there are sufficiently large PVDF single crystals of different phases (or single crystal films of sufficient thickness).

It should be noted that the difficulty of separating different phases of PVDF crystals by IR and Raman spectra has been established long ago [35], and it is primarily associated with the difficulty of obtaining samples of these polymers of sufficient crystallinity.

4. Conclusions

Analysis of the results of electronic structure calculations allowed us to obtain a number of conclusions about the peculiarities of the formation of electronic and optical properties of the α-, β-, and γ-phases of the PVDF crystal, as well as to make some predictions about the possibility of experimental monitoring of the phase composition of such compounds:

1) All three of these phases of the PVDF crystal are direct-band crystals.

2) For all three phases, there are no hydrogen H_s states in the energy region of the top of the Valence band, and the bottom of the Conduction band is dominated by carbon C_p states with a minor contribution from fluorine F_p and hydrogen H_s states.

3) All three phases of the PVDF crystal should have a hole type of conductivity. Their conductivity is essentially anisotropic, since the spatial movement of holes can only effectively occur in the direction of the carbon chains (crystallographic directions (1 0 0), (1 0 0), and (1 0 0) for α-, β-, and γ-phases, respectively).

4) X-ray diffraction experiments will allow to confidently distinguish the α- (or γ-) phase of a PVDF crystal from the β-phase of a compound, while distinguishing the α- from the γ-phase will be more difficult, although possible in principle.

5) The slight difference in refractive index values in the visible light spectral region suggests that the α-, β-, and γ-phases of the PVDF crystal will be extremely difficult to distinguish by experimental methods of surface ellipsometry.

6) Due to significant difference in the spectral position of the fundamental absorption edge (approximately 1 eV), the difference in the absorption spectra of the β- and α- (or γ-) phases of the PVDF crystal can be actually detected in reflectance experiments with use of vacuum ultraviolet light.

7) It will be practically impossible to distinguish between the α- and γ-phases of a PVDF crystal by experimental Raman spectroscopy in the Raman shift spectral region up to 1500 cm^{-1}. However, in such experiments, it will be easy to distinguish the β-phase from the $\alpha(\gamma)$-phase by the presence of intense Raman lines at 1072, 1174 and 1237 cm^{-1}.

8) The β-phase of a PVDF crystal can be easily distinguished from the $\alpha(\gamma)$-phase by means of IR absorption spectra by detecting spectral lines at 190 and 447 cm^{-1} .

1. T. Furukawa. Ferroelectric properties of vinylidene fluoride copolymers. *Phase Transitions* **18**, 143 (1989).
2. M.M. Alam, X. Crispin. The past, present, and future of piezoelectric fluoropolymers: Towards efficient and robust wearable nanogenerators. *Nano Research Energy* **2**, 4 (2023).
3. L. Lu, W. Ding, J. Liu, B. Yang. Flexible PVD F-based piezoelectric nanogenerators. *Nano Energy* **78**, 105251 (2020).
4. S.K. Karan, D. Mandal, B.B. Khatua. Self-powered flexible Fe-doped RGO/PVDF nanocomposite: An excellent material for a piezoelectric energy harvester. *Nanoscale* **7** (24), 10655 (2015).
5. F. Liu, N.A. Hashim, Y. Liu, M.R. Moghareh Abed, K. Li. Progress in the production and modification of PVDF membranes. *J. Membrane Science* **375**, 1 (2011).
6. S. Egusa, Z. Wang, N. Chocat, Z.M. Ruff, A.M. Stolyarov, D. Shemuly, Y. Fink. Multimaterial piezoelectric fibres. *Nature Materials* **9** (8), 643 (2010).
7. Z. Hu, M. Tian, B. Nysten, A.M. Jonas. Regular arrays of highly ordered ferroelectric polymer nanostructures for non-volatile low-voltage memories. *Nature Materials* **8** (1), 62 (2009).
8. S. Amer, W. Badawy. An integrated platform for bio-analysis and drug delivery. *Current Pharmaceutical Biotechnology* **6** (1), 57 (2005).
9. A. Heredia, M. Machado, I.K. Bdikin, J. Gracio, S. Yudin, V.M. Fridkin, A.L. Kholkin. Preferred deposition of phospholipids onto ferroelectric P(VDF-TrFE) films via polarization patterning. *J. Phys. D: Appl. Phys.* **43** (33), 335301 (2010).
10. S. Weinhold, M.H. Litt, J.B. Lando. Oriented phase III poly(vinylidene fluoride). *J. Polymer Sci.: Polymer Lett. Edit.* **17**, 585 (1979).
11. M. Li, H.J. Wondergem, M-J. Spijkman, K. Asadi, I. Katsouras, P.W.M. Blom, D.M. De Leeuw. Revisiting the δ-phase of poly(vinylidene fluoride) for solution-processed ferroelectric thin films. *Nature Materials* **12**, 433 (2013).
12. A.J. Lovinger. Annealing of poly(vinylidene fluoride) and formation of a fifth phase. *Macromolecules* **15**, 40 (1982).
13. W.M. Jr. Prest, D.J. Luca. The morphology and thermal response of high-temperature-crystallized poly(vinylidene fluoride). *J. Appl. Phys.* **46**, 4136 (1975).
14. R. Hasegawa, M. Kobayashi, H. Tadokoro. Molecular conformation and packing of poly(vinylidene fluoride). Stability of three crystalline forms and the effect of high pressure. *Polymer* **3**, 591 (1972).
15. V.V. Kochervinskii, B.V. Lokshin, S.P. Palto, G.N. Andreev, L.M. Blinov, N.N. Petukhova. Poly(vinylidene fluoride): Crystallization from solution and preparation of Langmuir films. *Vysokomolekulyarnye Soedineniya. Seriya A, Seriya B* **41**, 1290 (1999).
16. R. Hasegawa, Y. Tanabe, M. Kobayashi, H. Tadokoro, A. Sawaoka, N. Kawai. Structural studies of pressure-crystallized polymers. I. Heat treatment of oriented polymers under high pressure. *J. Polymer Sci. Part A-2: Polymer Phys.* **8**, 1073 (1970).
17. A.J. Lovinger. Crystallization and morphology of melt-solidified poly(vinylidene fluoride). *J. Polymer Sci. Polymer Phys. Edit.* **18**, 793 (1980).
18. S. Osaki, Y. Ishida. Effects of annealing and isothermal crystallization upon crystalline forms of poly(vinylidene fluoride). *J. Polymer Sci. Polymer Phys. Edit.* **13**, 1071 (1975).
19. G.T. Davis, J.E. McKinney, M.G. Broadhurst, S.C. Roth. Electric-field-induced phase changes in poly(vinylidene fluoride). *J. Appl. phys.* **49**, 4998 (1978).
20. R. Hasegawa, Y. Takahashi, Y. Chatani, H. Tadokoro. Crystal structures of three crystalline forms of poly(vinylidene fluoride). *Polymer* **3**, 600 (1972).
21. W.W. Doll, J.B. Lando. Polymorphism of poly(vinylidene fluoride). III The crystal structure of phase II. *J. Macromol. Sci. Part B: Physics* **4**, 309 (1970).
22. S. Enomoto, Y. Kawai, M. Sugita. Infrared spectrum of poly(vinylidene fluoride). *J. Polymer Scie. Part A-2: Polymer Phys.* **6**, 861 (1968).
23. A. Salimi, A.A. Yousefi. Conformational changes and phase transformation mechanisms in PVDF solution-cast films. *J. Polymer Sci. PART B: Polymer Phys.* **42**, 3487 (2004).
24. F.J. Boerio, J.L. Koenig. Vibrational analysis of poly(vinylidene fluoride). *J. Polymer Sci. Part A-2: Polymer Phys.* **9**, 1517 (1971).
25. A.M. Reyes, L. Sesenes, A. Mauricio. Effect of cationic substitution of metal species in poly(vinylidene difluoride)

($C_2H_2F_2$) by ab initio calculations. *Inorganic Chem.* **59** (2), 15189 (2020).

26. A. Itoh, Yo. Takahashi, T. Furukawa *et al.* Solid-state calculations of poly(vinylidene fluoride) using the hybrid DFT method: spontaneous polarization of polymorphs. *Polymer J.* **46** (4), 207 (2014).
27. V.S. Bystrov *et al.* Polarization of poly(vinylidene fluoride) and poly(vinylidene fluoride-trifluoroethylene) thin films revealed by emission spectroscopy with computational simulation during phase transition. *J. Appl. Phys.* **111** (10), 104113 (2012).
28. T.D. Huan, R. Ramprasad. Polymer structure prediction from first principles. *J. Phys. Chem. Lett.* **11** (15), 5823 (2020).
29. S.J. Clark, M.D. Segall, C.J. Pickard, P.J. Hasnip, M.J. Probert, K. Refson, M.C. Payne. First principles methods using CASTEP. *Zeitschrift Für kristallographie* **220** (5–6), 567 (2005).
30. K. Laasonen. Implementation of ultrasoft pseudopotentials in ab initio molecular dynamics. *Phys. Rev. B* **43** (8), 6796(R) (1991).
31. J.P. Perdew, K. Burke, M. Ernzerhof. Generalized gradient approximation made simple. *Phys. Rev. Lett.* **77** (18), 3865 (1996).
32. B.G. Pfrommer. Relaxation of crystals with the quasi-Newton method. *J. Computat. Phys.* **131** (2), 233 (1997).
33. Y. Hizhnyi. Origin of luminescence in $ZnMoO_4$ crystals: Insights from spectroscopic studies and electronic structure calculations. *J. Luminescence* **211**, 127 (2019).
34. J.M. Ziman. *Electrons and Phonons: The Theory of Transport Phenomena in Solids* (Oxford University Press, 1960).
35. M. Kobayashi, K. Tashiro, H. Tadokoro. Molecular vibrations of three crystal forms of poly (vinylidene fluoride). *Macromolecules* **8**, 158 (1975).

Received 19.09.24

З. Баранчиков, О. Макаренко,
С.Г. Недiлько, С.Г. Недiлько

ЕЛЕКТРОННА СТРУКТУРА ТА МОЖЛИВIСТЬ ЕКСПЕРИМЕНТАЛЬНОГО МОНIТОРИНГУ ФАЗОВОГО СКЛАДУ КРИСТАЛIВ ПОЛIВIНIЛIДЕНФТОРИДУ (PVDF)

Органiчний полiмер полiвiнiлiденфториду (PVDF) є перспективним та комерцiйно привабливим матерiалом для сучасних потреб нанотехнологiй i мiкроелектронiки та бiомедицини. Детектування фазового складу сумiшей PVDF є важливою технологiчною задачею. В роботi представлено результати *ab initio* розрахункiв електронної зонної структури трьох найбiльш розповсюджених фаз кристалiв полiвiнiлiденфториду, α-, β- та γ-PVDF. Одержано та проаналiзовано структуру одноелектронних зон, парцiальних густин електронних станiв, просторових розподiлiв електронної густини, спектрiв дiелекричних сталих, комплексного показника заломлення, поглинання та вiдбивання, спектри iнфрачервоного поглинання, комбiнацiйного розсiювання та рентґенограми α-, β- та γ-фаз PVDF. Проведений аналiз результатiв розрахункiв електронної структури дозволив зробити ряд висновкiв щодо особливостей формування електронних та оптичних властивостей α-, β- та γ-фаз кристала PVDF, а також зробити деякi передбачення щодо можливостi експериментального монiторингу фазового складу цiєї сполуки. Встановлено, що детектування одночасної наявностi β- та α-(або γ-) фази в зразках кристалiв PVDF може бути ефективно здiйснене методами спектроскопiї вiдбивання в дiапазонi вакуумного ультрафiолету, iнфрачервоного поглинання, комбiнацiйного розсiювання, рентґенофазного аналiзу. Видiлити ж наявнiсть α-фази на фонi γ-фази PVDF зазначеними методами буде практично неможливо.

Ключовi слова: полiвiнiлiденфторид, кристал, електронна структура, оптичнi спектри, фазовий склад.